ELSEVIER

International Journal of Mass Spectrometry 223–224 (2003) 447–458

International Journal of Mass Spectrometry

www.elsevier.com/locate/ijms

A three-step model applied to free electron attachment to C_{60}, Buckminsterfullerene

Matthias Lezius

Ion Physics Institute, Innsbruck University, Technikerstr. 125, Innsbruck A-6020, Austria

Received 25 January 2002; accepted 24 May 2002

Abstract

After a comparison of several experimental data sets, an analytical absolute cross-section for negative ion formation by low energy electron impact to C_{60} is derived. This cross-section is treated using a three-step model for electron attachment in which the electron is initially attracted by a polarizability potential with a Langevin capture rate, then it binds to the molecule after quantum mechanical energy transfer, and finally, following energy equilibration into vibrational modes, part of the electrons are lost due to auto-detachment. After removal of the Langevin and auto-detachment part from the experimental cross-section the energy dependent transition probability can be modelled by a series of Gaussian functions that are located at the allowed transition energies within the fullerene anion, thereby yielding the quantum mechanical transition probabilities. The transition probability can be compared to the density of valence states, if the electron affinity is correctly taken into account. This yields the energy dependence of the involved transition matrix elements. As a result, in C_{60} the transition matrix elements appear to be mostly independent of the transition, probably because Franck–Condon factors are of similar value over the entire energy range. (Int J Mass Spectrom 223–224 (2003) 447–458)

Keywords: Buckminsterfullerene; Electron; Attachment

1. Introduction

Under the aspect of free electron attachment reactions the anion formation of C_{60} Buckminsterfullerene represents a special exception, mainly because of two reasons. First, in contrast to many other molecules the formation of the non-fragmenting C_{60} anion is possible over a broad energy band from ∼0 up to above 10 eV, in other words non-dissociative electron attachment is possible even above the ionisation energy of the molecule. Second, because up to now the mother ion is the only observable anion, no negatively charged fragments of C_{60} have been found even at high primary electron energies up to 50 eV. The observable broad energy spectrum for ion formation appears immediately interesting, because usually upon electron attachment clearly distinguishable peaks are present. Such resonance-like features in electron attachment mostly stem from a few allowed transition energies between the initial neutral ground state and possible excited anion states. Qualitatively, the resonant behaviour, which is common to most electron attachment reactions, pictures the Franck–Condon overlap between the involved initial and final potential surfaces. However, as in most cases the anion surfaces tend to be of repulsive nature, the transitions will lead

E-mail: matthias.lezius@uibk.ac.at

1387-3806/02/$ – see front matter
PII S1387-3806(02)00871-0

to the production of negatively charged fragment ions, a situation that is often connected with quite significant broadening of the respective resonance. These fragmentation channels in (so-called) dissociative attachment reactions complicate the scientific analysis, because they multiply the number of the potential surfaces that are involved during anion formation. Even a relatively small molecule for electron attachment like SF_6 (often used as a reference standard) exhibits a respectable number of peaks, leading altogether to seven different fragment anions. Thus, compared to the rich complexity present already in few-atom molecules, C_{60} behaves very differently as it shows such a remarkable stability upon attachment, which projects the pathways for allowed energy transitions onto a well-known number of possible anion states of a single conformer. This fact should open opportunities for a much less elaborated evaluation, at least in relation to the number of constituents of the molecule.

Generally speaking, the family of quasi-spherical fullerene molecules like C_{60}, C_{70}, C_{82}, all seem to have a comparably large electron attachment cross-section that is reaching, or even exceeding, their geometrical size. This fact might be interesting for future applications, for example as an electron-trapping substance that would act in a similar way like SF_6, especially because of the exceptional chemical stability that fullerenes exhibit at very high temperatures. However, due to their low vapour pressures it is presently rather unlikely that fullerenes can immediately substitute SF_6.

At this point in time, a number of studies have been performed that were dedicated to measure the efficiency for electron attachment to C_{60} [1–10]. In these investigations the structure of the electron energy dependence for the fullerene anion formation between ∼0 and 20 eV was studied in detail with various experimental techniques. Some of the authors have assigned molecular transitions to prominent features in the attachment energy spectrum, often based on a more or less direct comparison with readily available data from electron energy loss spectroscopy (HREELS) [11–15] or photo-detachment (PD) [16–18]. In a few cases the results have also been scaled to obtain the absolute (experimental) attachment cross-section, using a calibration that was mostly based on a comparison with high precision flowing afterglow studies [19]. Nevertheless, some of the observed features in the attachment energy spectrum (which show up as enhancements on top of a broad, bulk-like, spectrum) appear to be inconsistent with HREELS data, or even with known states of the anion or of neutral fullerenes, depending on the interpretation of the authors. For example, the strong observable peak at around 1 eV is inconsistent with a known HOMO–LUMO gap of 1.5–2 eV [16]. Moreover, the broad resonance at around 6 eV has sometimes been attributed to π-plasmon excitations [2,4,8], sometimes to one-electron excitation [9,20]. Furthermore, there exists an ongoing discussion about the possibility of zero-energy attachment to the molecule, because in principle due to Renner–Teller splitting the necessary conditions for s-wave attachment are not met [21]. On the other hand, the majority of the experimental data shows a remarkably efficient anion production down to a few milli-electron volt [1–3,6–10], while in other data a shallow barrier has been observed [4,5,19]. It was recently suggested that temperature dependent electron–phonon coupling that would cause zero-energy attachment to vanish below a certain threshold temperature might cause such differences in observation. In conclusion it seems that there is still a need to clarify the situation concerning electron attachment to C_{60}, and in this sense the aim of the present work is two-fold. First, a fully analytical form of the cross-section will be provided that might turn out to be useful as an input for future simulations, for example for the simulation of a low temperature plasma containing C_{60} anions. Moreover, for the first time a semi-classical three-step model is introduced that appears capable to describe the electron attachment situation quantitatively well and that reaches excellent agreement between the available experimental data and some sophisticated ab initio calculations.

The strategy that will be used throughout the paper is as follows: in the first step a synthetic absolute electron capture cross-section σ_{att} (corresponding to the absolutely calibrated, experimentally observed ion

current) is derived from a comparison of several experiments. σ_{att} matches most of the data in the region from approximately 0 up to 10 eV. In a second step this cross-section is fitted and evaluated with respect to a three-step attachment model. Then, the result is compared and discussed in comparison with theoretical studies concerning the eigenstates and the density of states of the fullerene anion.

2. Electron capture cross-section of C_{60}

Based on a comparison of the experimental data provided by Elhamidi et al. [8], Jaffke et al. [2], Lezius et al. [1], and Smith and co-workers [5,19] the probability for the formation of fullerene anions upon electron attachment with primary electron energies between ∼0 and 10 eV can be obtained with quite reasonable accuracy. The analysis presented here will be primarily based on results provided by [2,8], who have independently obtained similar data. Consequently, based on these sets the relative energy dependence for ion production appears well reproducible. The relative dependence of the anion current can be absolutely calibrated using some recent absolute cross-sectional data from the region between 0 and 1 eV, which are based on neutral beam absorption measurements and have been provided by Kasperovic et al. [10]. It should be mentioned, that the very first free electron attachment to fullerenes was reported by the author himself [1], but this data deviates in the low energy region (0–3 eV), due to contaminative effects resulting from a Nier-type ion source used in that experiment. Close to zero electron energy Nier-type ion sources are known to become unable to keep important electron beam parameters constant (see for example [20]). Sometimes similar deviations from ideal working conditions are also present when electron monochromators are used (the deviation from ideal working conditions appears in a small energy band between 0 eV and the energy resolution of the device). In any case, electron monochromator data should be much more reliable for the low energy region. In contrast to the data reported by [2,8], the cross-section reported by Vostrikov et al. [6] shows a two-times stronger peak close to zero energy, leading to an over all disagreement of a factor two in the range between 0.5 and 10 eV compared to [2], because in [6] the absolute attachment cross-section close to zero energy was used for calibration. It should be noted that the data by [9] also shows strong zero-energy attachment that appears very similar to the observations in [6]. The (complementary) FALP data provided by Spanel and co-workers [19] uses a different approach, e.g., a thermalized low temperature plasma for the investigation of the attachment rate down to zero energy. Nevertheless, for whatever reason, the reported plasma rate constant does not indicate a significant cross-section at low electron temperatures. This fact is in contradiction to the quite large negative ion current at around zero electron energy that has been reported by several groups [1,8,9,22], and also in [5] (if the experimental data is interpreted differently according to [7]). Therefore, it will be assumed here that C_{60} with an internal temperature exceeding 600 K has no barrier upon electron attachment. Under this assumption, close to zero energy the electron attachment will have a comparably large cross-section, quite possibly following the observations of Kasperovic et al. [10], and in agreement with the strong signal that was also observed by [6,9]. In any case it is not really intended here, to interfere with the still ongoing discussion about the possibility of zero-energy attachment to fullerenes. Instead, the analysis presented here is mostly independent of the form of the cross-section close to zero energy, but concentrates instead on the form of the ion signal obtained above 100 meV up to approximately 10 eV. In this respect it should be noted that for electron energies at around 0.5 eV the reaction rate constant provided by Spanel and co-workers [19] seems to be in very reasonable agreement with the attachment cross-section of Kasperovic et al. [10] (unfortunately the data in [10] shows large error bars above 0.5 eV). Nevertheless, it is obvious that the outcome of the present analysis cannot be more accurate than the input data that was compiled from the different research groups. It is conservatively estimated that the analysis should

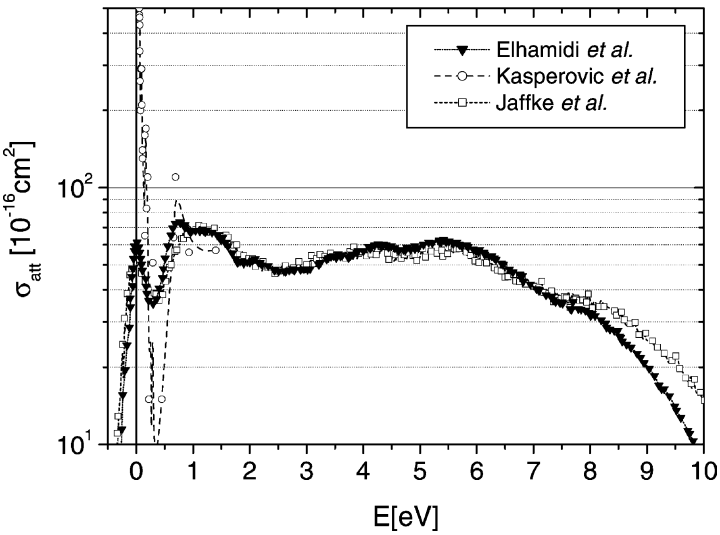

Fig. 1. Experimentally derived electron attachment cross-section σ_{att} of C_{60}, determined from a comparison between the experimental data of [2,8,10]. These data was used to construct the numerical cross-section used for further analysis and shown in Fig. 2.

have an absolute error of about 20% and a relative error of about 5% for the synthetic attachment rate σ_{att}. The complete dataset, which has been used under such considerations, is shown in Fig. 1. In this graph the absolute cross-section of [10], and the ion intensity data of [2,8] calibrated to that cross-section, are shown.

3. Evaluation with the three-step model

The data in Fig. 1 can be evaluated under the aspect of the following mechanism for electron attachment, based on three, essentially independent, steps:

1. Initial capture of the electron due to polarisation forces as suggested in [10,22]. The process is essentially controlled by the Langevin rate. In this model the electron is attracted by the polarizability α of C_{60}, in a Langevin-type process [23] with the cross-section given by (in cgs units):

$$\sigma_L(E) = \sqrt{\frac{2\pi^2 e^2 \alpha}{E}} \quad (1)$$

This cross-section models a pure classical capture of a particle with charge e, spiralling into the attractive potential of an infinitely small, polarizable, molecule. The attractive potential experienced by the incoming charged particle is given by $V(r) = -\alpha e^2/2r^4$. Note that the Langevin rate has been translated into a quantum mechanical picture by Vogt and Wannier [24], where the Langevin cross-section maintains and becomes a sum over all L-wave scattering probabilities, with L = s, p, d, f, ..., down to a correspondence limit of $(8\alpha E)^{1/4} \geq 1$ (in the case of C_{60} this limit appears to be at ~10 meV). As a pure classical collision cross-section the Langevin rate represents the upper limit for any point-charge attachment process to a polarizable, point-like, neutral particle. The Langevin cross-section is indicated in Fig. 2. However, the present molecule is not really a point-like target and the geometrical extension has to be taken into account. It can be assumed that C_{60} behaves very close to a perfectly conducting sphere of radius $R \sim 0.5$ nm, since all π-electrons are delocalised over the entire molecule. In such a case the cross-section should be modified (in a similar way this has been suggested recently for metal-clusters [25]), by adding a constant term that accounts for

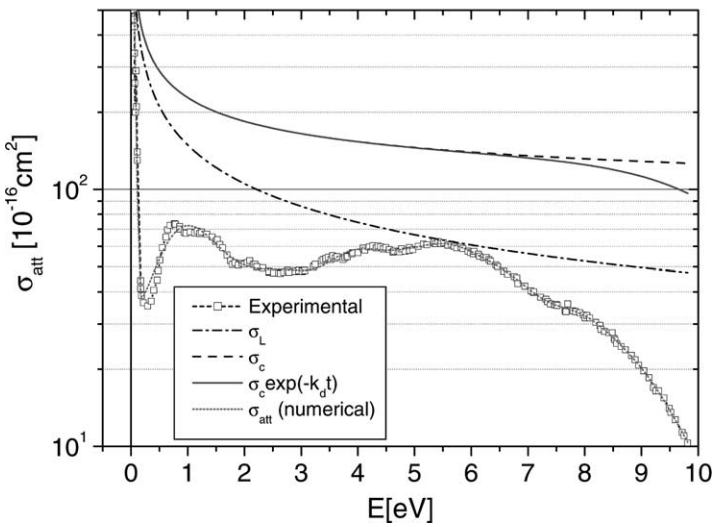

Fig. 2. Joined data of [8,10] and the fitted numerical curve σ_{att} used for the present analysis. Also indicated are the Langevin rate σ_L for the fullerene, the size corrected capture rate σ_c, and the capture rate after correction for auto-detachment $\sigma_c \exp(-k_d t)$, see text.

the geometrical size of C_{60} ($A = 79A^2$):

$$\sigma_c(E) = \sqrt{\frac{2\pi^2 e^2 \alpha}{E}} + A \quad (2)$$

The size corrected Langevin rate (for a polarizability of $78A^3$ as reported for C_{60} by [26,27]) will be called the classical capture cross-section σ_c, and is also indicated in Fig. 2. Most importantly, σ_c correctly exceeds the ion intensity data over the whole energy range. The classical capture cross-section represents all cases that are leading to an elastic or inelastic collision complex, regardless if final attachment happens or not. In principle, another term could be added that would account for the large hyperpolarizability of C_{60} [28]. However, in the analysis performed here the hyperpolarizability is not taken into account. First, because it can be assumed that it is screened efficiently [28], and second, because in the first approximation the energy dependence would only be modified by the addition of another comparably small constant in (2).

2. In the second phase of the attachment process the electron dives from a continuum state into a bound state via transfer of its primary electron energy into intramolecular excitation, i.e., the primary electron energy will be consumed by excitations of bound electron/nuclear states during anion formation. In the present study, any form of multi-electron excitation, like for example π-plasmon-excitation, is excluded and only direct electron–electron energy transfer is considered. Such a restriction is justified because an important selection rule for electron attachment processes is that always less than three electrons are directly excited during electron attachment [29]. In addition, in the present discussion possible continuum states of the final anion are considered to be unstable (and are therefore not detected experimentally). For this reason, only electronic excitations into long-lived bound states that are located below the Fermi-level (e.g., HOMO t_{1u} (−2.7 eV), HOMO + 1 t_{1g} (−1.65 eV), HOMO + 2 t_{2u} (−0.65 eV), HOMO + 3 h_g (−0.55 eV)) are taken into account. These direct electron–electron excitations are controlled by quantum mechanical transition probabilities. The energy dependence of such transition probabilities can be estimated using Fermi's golden rule, giving a probability $w_{a\to b} \cong (2\pi/\hbar)|V_{ba}|^2 \rho_b$ for the transition

between the initial energy E_a and the final energy E_b in a quantum system (see, e.g., [30]). The coefficient V_{ba} represents the transition matrix element and ρ_b corresponds to the density of states (DOS) of the final state b. It will be shown here that it appears indeed possible to gather useful information about the matrix elements V_{ba} from an evaluation of the experimentally derived electron attachment data. A more detailed explanation how the density of states is linked to the attachment cross-section will be given in detail further below.

3. In the third step subsequent losses of anions in the experiment are taken into account. The energy dependent part of signal losses is mainly due to auto-detachment (or thermionic emission) [31], which has reportedly a strong influence on the high-energy tail of the experimental signal [5]. Loss of the negative charge happens within the time window t from ionisation to ion detection, and it becomes much more probable for higher initial electron energies, in the case of C_{60} especially above 8 eV. The survival probability for the ions during their flight time from the ionisation to detection is given by $P_s = N(t)/N(0) = \exp(-k_d t)$, where $N(t)$ denotes the total number of ions present at time t. As described in detail in [5], the unimolecular detachment coefficient can be presented using an Arrhenius law: $k_d = A_d \exp(-E_A/k_b T)$. Here, $A_d = 2.5 \times 10^{11}\ s^{-1}$ is the Arrhenius coefficient (value is taken from [5]), E_A is the electron affinity (for C_{60} a value of $E_A \approx 2.68$ eV has been reported by several groups [16–18]), k_b is the Boltzmann constant, and T is the internal temperature of the fullerene anion. The internal temperature of the fullerene anion has to be derived from the evaporation temperature T_{evap}, the primary electron energy E, and the electron affinity E_A. For the energy region of interest the determination of the temperature, as given in curve a, Fig. 2 in [5], can be approximated using a simple linear fit: $T = T_{evap} + 68(E_A + E)$, where energies are given in electron volt, and temperatures in Kelvin. Fig. 2 shows the modification of the capture cross-section when auto-detachment at an evaporation temperature of 750 K is taken into account (the flight time t was assumed to be 300 μs).

An important goal of this work is to gather information about Step 2. However, before one can proceed to compare the experimental data with ab initio calculations, the primary Langevin rate of Step 1 has to be taken into account, and also the losses in the highly energetic tail due to auto-detachment caused by Step 3. It is assumed that the situation is based on a pure sequential, and therefore physically independent series of processes. Therefore, the total probability for the detection of anions (which is proportional to the ion current from ρ_{tot}) will be given by the product of all partial probabilities that are involved: the capture probability P_c (1), the transition probability P_T (2), the survival probability P_s (3) and the detection probability P_{det} (4):

$$\sigma_{att} \propto P_c P_T P_s P_{det} \propto \sigma_c(E) \times \left[\sum_{a,b} \frac{2\pi}{\hbar} |V_{ba}(E)|^2 \rho_b(E) \right] \exp(-k_d t) P_{det} \quad (3)$$

The detection probability P_{det} will be (mostly) independent of the primary electron energy E, if we assume that the internal energy of the molecule cannot be converted efficiently on the surface of the detector dynode. In other words, it is assumed that the internal energy of C_{60} is negligible compared to the kinetic energy upon detection. Suppressing all constant terms reduces Eq. (3) to

$$\sum_{a,b} \frac{2\pi}{\hbar} |V_{ba}(E)|^2 \rho_b(E) \propto P_T \propto \frac{\sigma_{att}}{\sigma_c \exp(-k_d t)} \quad (4)$$

It is now suggested that the left side of (4) can be modelled as a sum over Gaussian functions, which are located at the allowed transition energies between the different bound states of the anion $E_b - E_a$, each having a width (FWHM) of $2\delta_{a\to b}$:

$$\sum_{a,b} \frac{2\pi}{\hbar} |V_{ba}(E)|^2 \rho_b(E) \approx \sum_{a\to b} \frac{A_{a\to b}}{\sqrt{2\pi\delta^2_{a\to b}}} \exp\left(-\frac{(E_b - E_a)^2}{2\delta^2_{a\to b}} \right) \quad (5)$$

For the one-electron electronic transitions in thermally hot C_{60} the width of these transitions should be, in a first order, fairly independent of the initial and the final state ($\delta_{a\rightarrow b} \equiv \delta$). Due to the geometry of the fullerene molecule and the perfect delocalisation of all π-bonding electrons over the entire molecule, vibrational broadening affects all electronic states similarly. Therefore, it can be assumed that the internal temperature of the molecule causes similar thermal broadening to all levels, at least as long as molecular dissociation does not happen (note that fragment anions are not observed for C_{60}). Here, δ is set to 0.5 eV (several values for δ have been tested during the numerical evaluation and the χ^2-error of the fit showed a minimum at ∼0.55 eV). This δ corresponds well to the slope of the experimental cross-section between 0.5 and 1 eV, indicating a thermal broadening of approximately 1 eV (FWHM). For the numerical evaluation the theoretically derived eigenstates of the C_{60} anion provided by Wästberg and Rosen [32] (applying a DV-SCC ab initio technique) are used. The states in [32] are in excellent agreement with various experimental works [11,12,16]. All possible valid combinations for electron transitions within the molecule are taken into account. This means that most combinations between initial and final anion states are admitted, as long as 'b' can be assumed to be initially non-occupied and below the boundary limit, e.g., of the form HOMO+n, $n = 1$–3. The suppression of any other selection rule is justified by two reasons: first, only a few selection rules apply to electron attachment (change of spin $S \rightarrow |S \pm (1/2)|$, direct excitation of less than three electrons, and change of molecular symmetry $\Sigma^{\pm} \rightarrow \Sigma^{\mp}$ [29]) and cases have been observed when they are weakened due to changes in the molecular geometry, for example after condensation [33]. Second, it can be assumed that any further restriction by selection rules will naturally show up in the present analysis of the experimental data in form of small or negligible amplitudes $A_{a\rightarrow b}$. In sum 50 transition energies between ∼0 and 14 eV are used, e.g., the right side of (5) is presented by a sum over 50 Gaussian functions with equal FWHM widths of approximately 1.0 eV. Only for the lowest attachment energy (at ∼0 eV), the width has been reduced to 0.1 eV. This small width close to ∼0 eV is justified because zero electron energy attachment (s-wave attachment) tends to produce very narrow experimental peaks that follow a dependency

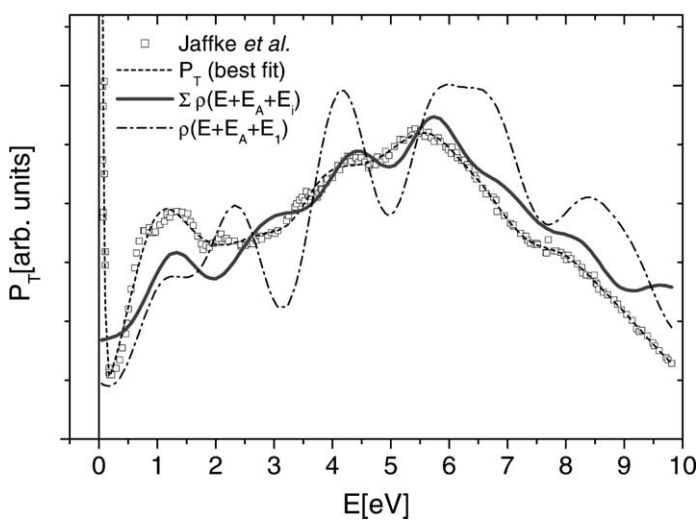

Fig. 3. The synthetic cross-section taken from Fig. 2, when corrected for the absolute collision cross-section and for auto-detachment (see Eqs. (3) and (4), and text). This curve represents the transition probability P_T for formation of a bound, long-lived, C_{60}^-. Also shown for comparison is the energetically shifted density of states based on ab initio calculations by [32], and a superposition of two energetically shifted densities $\rho_{tot}(E)$, see text.

like $\sigma = (\pi/2E)/(1 - e^{-4\sqrt{2\alpha E}})$ [34]. It should be mentioned that in the case of strong auto-detachment zero energy peaks would become even narrower. To fit the amplitudes of the Gaussian functions to the experimental data a non-linear Levenberg–Marquart algorithm is applied [35]. With this technique in most cases already after 10 iterations a nearly perfect agreement to the experiment can be achieved. Nevertheless, all coefficients given here have been calculated with at least 30 iterations. Fig. 3 shows the experimental data (corresponding to the right side of Eq. (4)), compared to the fitted curve P_T (corresponding to the right side of Eq. (5)). The covariance matrix of the coefficients (not shown) indicates that the A_i obtained in this manner are not independent of each other. This is reasonable, because 50 Gaussian functions with an FWHM of 1 eV in the interval from 0 to 14 eV have a significant overlap. To test for covariance effects the order of the initial values of the parameters was additionally randomised, so that adjacent Gaussian peaks had largely different indices. However, randomisation showed no significant effect on the numerical result.

4. Comparison and discussion

The sharp resonance of P_T at ~0 eV, visible in Fig. 3, is caused by the strong rise of the ion signal in this region that was reported by [10] and that has been included in the present evaluation. Such strong enhancement of P_T at zero energy vanishes completely for the case that the original data-points of Elhamidi et al. [8], or Jaffke et al. [2], are used instead of the numerical cross-section shown in Fig. 2. Apart from the sharp and strong zero energy peak the dependence of P_T shows a very broad, triangular shaped, form that reaches its maximum at around 6 eV. The most prominent features are extended and super positioned signal enhancements located at approximately 1.4, 4.4, 5.5 and 8.0 eV, each of these features is extending over about 2 eV. It is interesting to note that apart from the zero energy peak all features are observable in a similar way if the data is compiled from different experiments, even if the electron resolution was quite different in these studies. Moreover, due to the monotonously increasing character of the correction factor $1/P_cP_s$ used in Eq. (4), the same features are also clearly visible in the direct ion current data (see Figs. 1 and 2). As mentioned above, the appearance of broad and only slightly structured continua appears to be a common feature to most fullerenes. Probably the only hope to achieve an increased contrast between the observable resonances would be the use of a beam of very cold C_{60}. Up to now, however, a cold beam technique has not been applied by any of the involved research groups to fullerenes.

Most of the previous authors have compared the observable structures to HREELS or PD. Regarding such a comparison, the author deeply believes that this can lead to significant confusion and misinterpretation, and the reasons for this can be easily understood. In HREELS, the eigenstates of a neutral C_{60} molecule are monitored, because part of the initial electron energy is deposited into a finally neutral system. During electron attachment (EA), however, in addition the electron affinity energy is available, and therefore HREELS and EA cannot be compared in a direct manner, at least not without taking the (adiabatic) electron affinity into account. On the other hand, with PD the density of states of the anion is correctly observed. In this respect it should be noted that in Fig. 4 of [32] the density of states was directly compared to PD measurements. Nevertheless, once again the electron affinity (which shows up as the minimum photon energy at which neutralisation of C_{60} is observed in PD) will energetically shift all electron attachment features quite considerably compared to observable peaks in PD. Moreover, in most cases PD studies have been performed on long-lived (ground state) C_{60} anions. Complementary to this, excited eigenstates above the HOMO-level of C_{60}^- have been confirmed experimentally using inverse photo-emission [36].

As a conclusion, instead of comparing HREELS and PD directly to EA the author suggests that the following approach should be considered, which is schematically shown in Fig. 5. When the electron with initial energy E comes into vicinity of the fullerene, it will, for a very short time (probably less than the

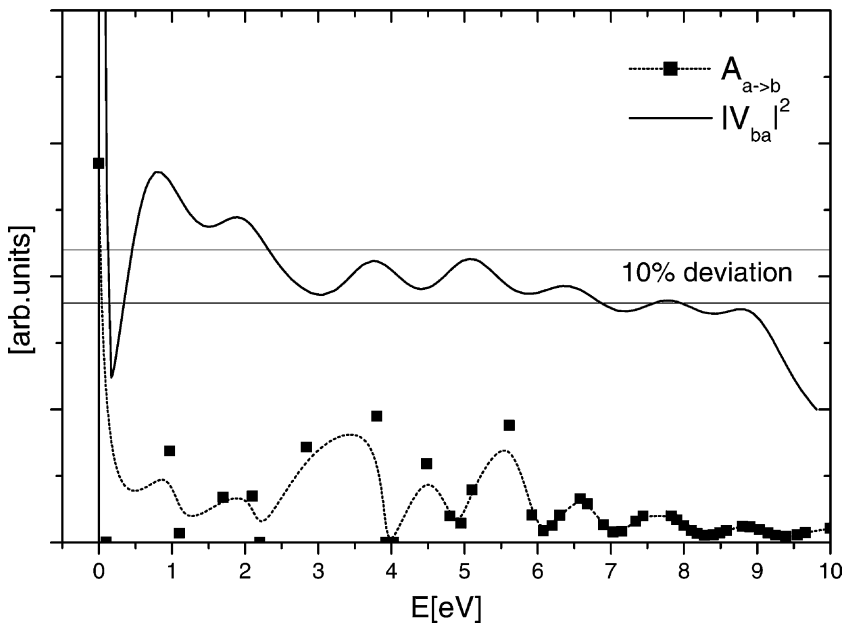

Fig. 4. The transition probability P_T, divided by the superimposed density of states $\rho_{tot}(E)$, as shown in Fig. 3. The deviation of the curves from each other is in the order of ±10%. P_T was fitted with a series of Gaussian functions (following Eq. (5)) with individual amplitudes $A_{a\to b}$ and similar widths $\delta = 0.5$ eV. The amplitudes and the energetic positions of the coefficients $A_{a\to b}$, which are also listed in Table 1, are indicated.

transient time of the electron, because the attachment cross-section is so large), form an anion that is in an excited continuum state. From this transient state the electron dives into a bound state. This will be presumably the HOMO level of the anion, sitting at the lowest available energy of −2.68 eV (=$-E_A$, below the vacuum level). Consequently, the total energy that is now available to the molecule should be $\tilde{E} = E + E_A$. This (considerable) energy can be rapidly transferred into electronic excitation (corresponding to an Auger-like process), or on a somewhat longer timescale into nuclear excitation. If we assume that electronic excitation dominates the very early period, one electron below the HOMO-level will be excited into HOMO + 1, HOMO + 2, etc. (In principle, double population of the HOMO-level of the anion is also possible. But it will be at least 50% less probable than excitation into the higher levels and is therefore not taken into account here.) This means that when applying the golden rule the DOS ρ is projected onto these eigenstates with the corresponding transition matrix elements. For example, if one is to assume that only one additional level at HOMO + 1 with energy E_1 (where E_1 is negative with respect to the vacuum level) would be available in the molecule, the energy dependence for the attachment efficiency should roughly follow the dependence $\rho(\tilde{E} - E_1)$. In other words the curve ρ has to be shifted towards lower energies E by the electron affinity, and, in addition, by the difference between the vacuum level and E_1. However, in C_{60} two binding energies are accessible for an Auger electron, at −1.65 eV (HOMO + 1) and at approximately −0.6 eV (HOMO + 2 and HOMO + 3 are so close that they can be treated as one level here). In this case the attachment efficiency should therefore roughly follow the dependence $\rho_{tot}(E) = \rho(\tilde{E} - E_1) + \rho(\tilde{E} - E_2)$.

Fortunately, the theoretical DOS ρ for the anion of C_{60} has been derived by [32] (in a much more elaborated method compared to [37]), using a FWHM of about 0.8 eV for all peaks. Here, their result has been

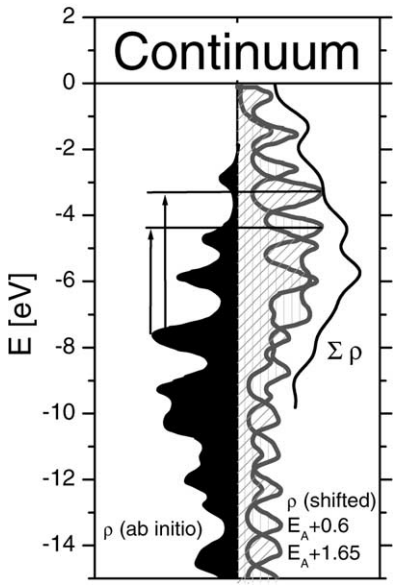

Fig. 5. Schematic presentation of the method to derive comparison between the density of states and the transition probability. The density of states of the anion (left side, [32]) was shifted by the electron affinity (2.68 eV) and the position of the accessible bound states HOMO + 2 (∼1.65 eV) and HOMO + 3–4 (∼0.6 eV). The sum of both densities is then calculated to produce a superimposed $\rho_{tot} = \sum \rho$, which was in the present case directly compared to the transition probability P_T (see Fig. 3).

Table 1
Transition energies $E_b - E_a$ and coefficients $A_{a\to b}$ obtained from fitting of the transition probability P_T with a sum of Gaussian functions of width $\delta = 0.5$ eV (apart from $i = 1$, 2 where the width was assumed to be 0.1 eV)

i	$E_b - E_a$	$A_{a\to b}$	i	$E_b - E_a$	$A_{a\to b}$
1	0	1.288	26	7.34	0.038
2	0.1	0.009	27	7.44	0.049
3	0.97	0.269	28	7.83	0.047
4	1.1	0	29	7.9	0.04
5	1.7	0.098	30	8	0.029
6	2.1	0.114	31	8.1	0.02
7	2.2	0	32	8.18	0.014
8	2.84	0.203	33	8.28	0.011
9	3.8	0.261	34	8.4	0.013
10	3.92	0	35	8.49	0.017
11	4.03	0	36	8.58	0.021
12	4.48	0.149	37	8.8	0.028
13	4.8	0.058	38	8.9	0.026
14	4.95	0.038	39	9.03	0.021
15	5.1	0.097	40	9.15	0.015
16	5.61	0.222	41	9.25	0.011
17	5.92	0.05	42	9.39	0.01
18	6.08	0.02	43	9.55	0.014
19	6.2	0.03	44	9.66	0.019
20	6.3	0.05	45	10	0.023
21	6.58	0.082	46	10.1	0.018
22	6.68	0.071	47	10.35	0
23	6.9	0.031	48	10.45	0
24	7.03	0.017	49	10.53	0
25	7.15	0.018	50	10.8	0.031

Values have been derived from evaluation of the experimental data using Eqs. (4) and (5) in connection with a Levenberg–Marquart algorithm (see text).

modified in a way that first all peaks are broadened to a FWHM of 1 eV. Then, ρ has been two times superimposed, one time shifted by $E_A + 1.65$ eV and one time shifted by $E_A + 0.6$ eV. The procedure is schematically shown in Fig. 5. The resulting curve $\rho_{tot}(E)$ is shown in Fig. 3, and the similarity between P_T and the superimposed and shifted $\rho_{tot}(E)$ is quite impressive. Within the energy interval of 2–9 eV both curves agree about 10%. Moreover, ρ_{tot} shows comparable features at 1.3, 4.4, 5.7, and 8.2 eV. In the opinion of the author the overall agreement is quite satisfactory. It should be noted that such an agreement couldn't be achieved if only one energy level (HOMO + 1 or HOMO + 2) is taken into account. In such a case, also shown in Fig. 3 for comparison, the overall agreement with the experimental data is much worse and the observable features seem to appear at very different energies. With respect to the golden rule, the overall agreement between P_T and ρ_{tot} indicates that the matrix elements $|V_{ab}|^2$ have approximately the same value; they seem to be mostly independent of the transition energy. This can be interpreted in a sense that, as already mentioned, all π-electrons in C_{60} are fully delocalised over the entire molecule. This provides a comparable Franck–Condon overlap between all states.

The amplitudes and energies of the coefficients $A_{a\to b}$ obtained from the fitting algorithm are indicated in Fig. 4 and summarised in Table 1. With these values it is immediately possible to reconstruct $\rho_{tot}(E)$ numerically when using Eqs. (4) and (5). The values of the coefficients are well within the same order of magnitude and indicate once more that the transition probabilities between completely different

states and for quite different energies apparently do not vary by more than a factor 5 (apart from three apparently forbidden transitions at 1.0, 2.3 and 4.0 eV most coefficients have a value between 0.1 and 0.5). Nevertheless, the coefficients $A_{a\rightarrow b}$ seem to exhibit at least some oscillatory dependence on the energy, with a frequency approaching 1 eV, more prominent for primary electron energies above 4 eV. At the present stage it is not clear to the author if these oscillations are of true physical origin. They could be caused by (less strict) selection rules and/or by slight variations of the Franck–Condon overlap. On the other hand, the fitting algorithm itself can give reason for an oscillatory behaviour. Due to the restricted use of a fixed $\delta_{a\rightarrow b}$, and an unavoidable non-vanishing covariance (caused by the thermal broadening) it is suggested here that these oscillations should not be over-interpreted at the moment.

It is possible to calculate the ratio between ρ_{tot} and the fitted curve for P_T. This yields direct information about the energy dependence of the transition matrix elements $|V_{ba}|^2$. The result obtained after the division P_T/ρ_{tot} is indicated as a full line in Fig. 4. The curve oscillates around a value of 1 between 1 and 10 eV. Below 1 eV and above 10 eV the deviations are stronger and indicate failure of the approach. This is reasonable in both cases. Below 1 eV the attachment process possibly changes towards a nuclear excited resonance, e.g., the primary electron energy is transferred into nuclear excitation rather than electron excitation. Above 8 eV auto-detachment and electron impact ionisation open as new reaction channels, which can strongly affect the efficiency for anion formation.

5. Conclusion

The present re-compilation of the experimental data available for electron attachment to C_{60} leads to a number of interesting results. First, a semi-classical three-step model has been successfully applied for electron attachment to fullerenes. This three-step model is based on an initial pure classical trapping reaction, a secondary quantum mechanical transition into a bound state and (after energy equilibration) an auto-detachment reaction based on a classical, Boltzmann-statistical, mechanism. Because such a three-step model appears capable to describe electron attachment to fullerenes well, it could perhaps be possible to generalise it to other attachment reactions. However, an important ingredient for the success of the present model was the stability of the C_{60} anion upon fragmentation up to large electron energies. Because fragmentation of the anion (e.g., dissociative attachment) is the more general case, the splitting of the transition matrix elements into several pathways will unfortunately complicate the analysis in other situations immediately. Nevertheless, concerning the general applicability of the model, it probably still applies to a lot of cases, not only to fullerenes. Many large and symmetric molecules have not been studied at this point in time (mostly due to the low vapour pressure of these molecules). In general, whether or not non-dissociative electron attachment is seen at high energies is related to the availability of empty orbitals, lifetimes and the absence of dissociation (although in many times auto-detachment and dissociation can compete). It is well known that auto-detachment due to thermionic emission is a general feature for molecules, for example the classic case of $e + SF_6 \Leftrightarrow SF_6^{*-}$ can be regarded as thermionic emission (for a review on thermionic emission from small aggregates see for example [38]). In addition, also the Langevin capture model is a very general approach that models the initial formation of the electron–molecule collision complex quantitatively well. This suggests that for a correct treatment of experimental electron attachment data the Langevin capture rate and the thermionic emission rate should always be taken into account.

On the other hand, due to the special electronic character of fullerenes the treatment of the second step, as performed here, is much less general. At least, in the common case one should be very careful to assume similar values for the Franck–Condon overlap over the entire density of states. Nevertheless, today for many anions the eigenstates, the matrix

elements, and the transition probabilities, can be calculated with reasonable accuracy. Thus, perhaps many molecules exist where the present scheme could be successfully applied with some minor modifications. Apart from the three-step model it appears very encouraging that the quite complex shape of the experimental electron attachment data is indeed closely related to ρ_{tot}. The direct comparison between the experimental P_T and the sum over a few energetically shifted DOS has lead to an excellent agreement that is better than 10% over an impressive energy range of 7 eV.

Acknowledgements

This work is dedicated to Prof. W. Lindinger, who introduced me to the concept of the Langevin model at the University of Innsbruck. His sudden death leaves an empty space, in the Institute for Ion Physics, and in the associated scientific community. The author gratefully acknowledges the substantial critique from one of the referees, which has contributed significantly to the present form of the article.

References

[1] M. Lezius, P. Scheier, T. Märk, Chem. Phys. Lett. 203 (1993) 232.
[2] T. Jaffke, E. Illenberger, M. Lezius, S. Matejcik, D. Smith, T.D. Märk, Chem. Phys. Lett. 226 (1994) 213.
[3] C.D. Finch, R.A. Popple, P. Nordlander, F.B. Dunning, Chem. Phys. Lett. 244 (1995) 345.
[4] J. Huang, H.S. Carman, R.N. Compton, J. Phys. Chem. 99 (1995) 1719.
[5] S. Matejcik, T.D. Märk, P. Spanel, D. Smith, T. Jaffke, E. Illenberger, J. Chem. Phys. 102 (1995) 2516.
[6] A. Vostrikov, D.Y. Dubov, A.A. Agarkov, Technol. Phys. Lett. 21 (1995) 517.
[7] J.M. Weber, M.W. Ruf, H. Hotop, Zeitschrift Phys. D 37 (1996) 351.
[8] O. Elhamidi, J. Pommier, R. Abouaf, J. Phys. B: Atom, Mol. Opt. Phys. 30 (1997) 4633.
[9] J. Vasilev, R.F. Tuktarov, V. Mazunov, Rapid Commun. Mass Spectrom. 11 (1997) 757.
[10] V. Kasperovic, G. Tikhonov, V.V. Kresin, Chem. Phys. Lett. 337 (2001) 55.
[11] G. Gensterblum, J.J. Pireaux, P.A. Thiry, J.P. Vigneron, P. Lambin, A.A. Lucas, Phys. Rev. Lett. 67 (1991) 2171.
[12] D.L. Lichtenberger, K.W. Nebesny, C.D. Ray, Chem. Phys. Lett. 176 (1991) 203.
[13] J.W. Keller, M.A. Coplan, Chem. Phys. Lett. 193 (1992) 89.
[14] A.W. Burose, T. Dresch, A.M.G. Ding, Zeitschrift Phys. D: Atoms Molecules Clusters 26 (1993) 294.
[15] A. Ding, in: L.A. Morgan, H. Ehrhard (Eds.), Electron Scattering by Molecules, Clusters and Surfaces, Plenum Press, London, 1993.
[16] S.H. Yang, C.L. Pettiette, J. Conceicao, O. Cheshnovsky, R.E. Smalley, Chem. Phys. Lett. 139 (1987) 233.
[17] L.-S. Wang, J. Conceicao, C. Jin, R.E. Smalley, Chem. Phys. Lett. 182 (1991) 1.
[18] C. Brink, L.H. Andersen, P. Hvelplund, D. Mathur, J.D. Volstad, Chem. Phys. Lett. 233 (1995) 52.
[19] D. Smith, P. Spanel, T.D. Märk, Chem. Phys. Lett. 213 (1993) 202.
[20] M. Lezius, T. Rauth, V. Grill, M. Foltin, T.D. Märk, Zeitschrift Phys. D 24 (1992) 289.
[21] E. Tosatti, N. Manini, Chem. Phys. Lett. 223 (1994) 61.
[22] I.I. Fabrikant, H. Hotop, Phys. Rev. A 63 (2001) 022706/1.
[23] P. Langevin, Ann. Chim. Phys. 5 (1905) 245.
[24] E. Vogt, G.H. Wannier, Phys. Rev. 95 (1954) 1190.
[25] V. Kasperovic, Phys. Rev. Lett. 85 (2000) 2729.
[26] R. Antoine, P. Dugourd, D. Rayane, E. Benichou, M. Broyer, F. Chandezon, C. Guet, J. Chem. Phys. 110 (1999) 9771.
[27] A. Ballard, K. Bonin, J. Louderback, J. Chem. Phys. 113 (2000) 5732.
[28] Y. Wang, G.F. Bertsch, D. Tomanek, Zeitschrift Phys. D 25 (1993) 181.
[29] H. Sambe, D.E. Ramaker, Phys. Rev. A 40 (1989) 3651.
[30] A. Messiah, Quantenmechanik, Walter de Gruyter, Berlin, New York, 1985.
[31] C. Yeretzian, K. Hansen, R.L. Whetten, Science 260 (1993) 652.
[32] B. Wästberg, A. Rosen, Phys. Scripta 44 (1991) 276.
[33] R. Azria, L. Parentau, L. Sanche, Phys. Rev. Lett. 59 (1987) 638.
[34] C.E. Klots, Chem. Phys. Lett. 38 (1976) 61.
[35] D.W. Marquardt, J. Soc. Ind. Appl. Math. 11 (1963) 431.
[36] M.B. Jost, N. Troullier, D.M. Poirier, J.L. Martins, J.H. Weaver, L.P.F. Chibante, R.E. Smalley, Phys. Rev. B 44 (1991) 1966.
[37] K. Tanaka, M. Okada, K. Okahara, T. Yamambe, Chem. Phys. Lett. 193 (1992) 101.
[38] C.E. Klots, Chem. Phys. Lett. 38 (1996) 61.